Phase Defects as a Measure of Disorder in Traveling-Wave Convection

A. La Porta and C. M. Surko
Department of Physics, University of California, San Diego, La Jolla, California 92093
(Received 3 May 1996)

Spatiotemporal disorder is studied in traveling-wave convection in an ethanol-water mixture. A technique for calculating the complex order parameter of the pattern is described, and the identification of phase defects is demonstrated. Point defects, domain boundaries, and standing wave patterns are shown to produce unique defect structures. The transition from a disordered state to a more ordered pattern is described in terms of the dynamics of defects and their statistics. [S0031-9007(96)01282-3]

PACS numbers: 47.27.Te, 47.52.+j, 47.54.+r

When a homogeneous, spatially extended system is driven far from equilibrium, a breaking of translational symmetry often occurs, which results in the formation of a pattern. Examples include the formation of convection rolls in a fluid layer heated from below and the formation of chemical waves in reaction-diffusion systems. In contrast to equilibrium systems, which are governed by a free-energy minimization principle, patterns in nonequilibrium systems typically exhibit nonrelaxational dynamics. This allows a much richer variety of patterns and makes a general understanding of the pattern selection mechanisms in nonequilibrium systems very difficult.

In some cases, especially when the patterns have a relatively simple spatial or temporal structure and when the systems are not driven far beyond their primary instability, the patterns are universal and are determined by the symmetries of the system [1]. Recent work has extended the search for universal phenomena to systems exhibiting spatiotemporal disorder, in which the patterns vary in time and space in a complicated manner.

Spatiotemporal disorder can involve the chaotic evolution of an amplitude field [2,3], or it can be more closely connected with the dynamics of defects. Defect chaos has been investigated in a variety of nonequilibrium physical systems [4–6] and in patterns generated by mathematical models [7–9]. Spectral techniques, based on the spatial Fourier transform or correlation function, are often used to characterize the degree of disorder in such patterns [10], but these linear measures are often not sufficient to describe strongly nonlinear systems. There is a clear need for a practical means of characterizing defect chaos in experimental patterns.

In this Letter we describe an investigation of defect-mediated spatiotemporal chaos in a strongly nonlinear traveling-wave (TW) state which occurs in binary fluid convection at large negative separation ratio. We present a technique for calculating the complex order parameter from the experimental TW patterns which allows us to identify phase defects and record their trajectories during the evolution of a pattern. We show that tracking the statistics of the defects is an effective way to characterize the transition from a highly disordered state to a more regular pattern.

The convection experiment was performed in a solution of 8% ethanol (by weight) in water at a mean temperature of 26 °C. The forcing parameter is the Rayleigh number, which is proportional to the temperature difference imposed on the fluid layer. In ethanol-water mixtures the Soret effect results in a coupling of the ethanol concentration to the temperature gradient that is parametrized by the separation ratio, ψ. The system is also characterized by the Prandtl number Pr which is the ratio of viscosity and thermal diffusivity and the Lewis number $\mathcal{L}$, which is the ratio of solute diffusivity to thermal diffusivity [1]. In the experiments described here, $\psi = -0.24$, $\mathcal{L} \approx 10^{-2}$, and $\mathrm{Pr} = 10.5$. For these parameters the onset of convection is a subcritical Hopf bifurcation to a state of oscillatory convection, which subsequently evolves to a state of continuously overturning traveling-wave convection [11]. This is a strongly nonlinear state in which the amplitude of convection is saturated, and rolls propagate with a well defined phase velocity.

The experiments described here were performed just above the saddle node [12], at $R/R_c = 1.27$ (where $R_c = 1708$ is the critical Rayleigh number of a pure fluid). The cylindrical convection cell consists of a sapphire top plate and a polished silicon bottom plate. It has a diameter of 24 cm and a height of $h = 0.4$ cm. Below, distances are expressed in terms of h, and times are expressed in terms of the vertical thermal diffusion time, $\tau = 124$ s. Patterns are visualized using a white light shadowgraph and are recorded with a charge coupled device camera and a frame grabber for computer analysis. A detailed description of the apparatus and the physical parameters of the experiment has been published elsewhere [12].

In order to initiate a maximally disordered convection pattern, the Rayleigh number is rapidly increased to a high value ($\approx 2.5R_c$), then set to the final value of $1.27R_c$ after the onset of convection is observed. Following a brief transient of about 20τ, the pattern settles into a state of persistent spatiotemporal disorder, which typically lasts for 1000τ. An example of a disordered convection pattern containing numerous small domains of traveling waves, standing waves, sources, and dislocations is shown in Fig. 1(a). The disordered pattern then undergoes a transition to a much more regular traveling-wave pattern,

 0031-9007/96/77(13)/2678(4)$10.00 © 1996 The American Physical Society

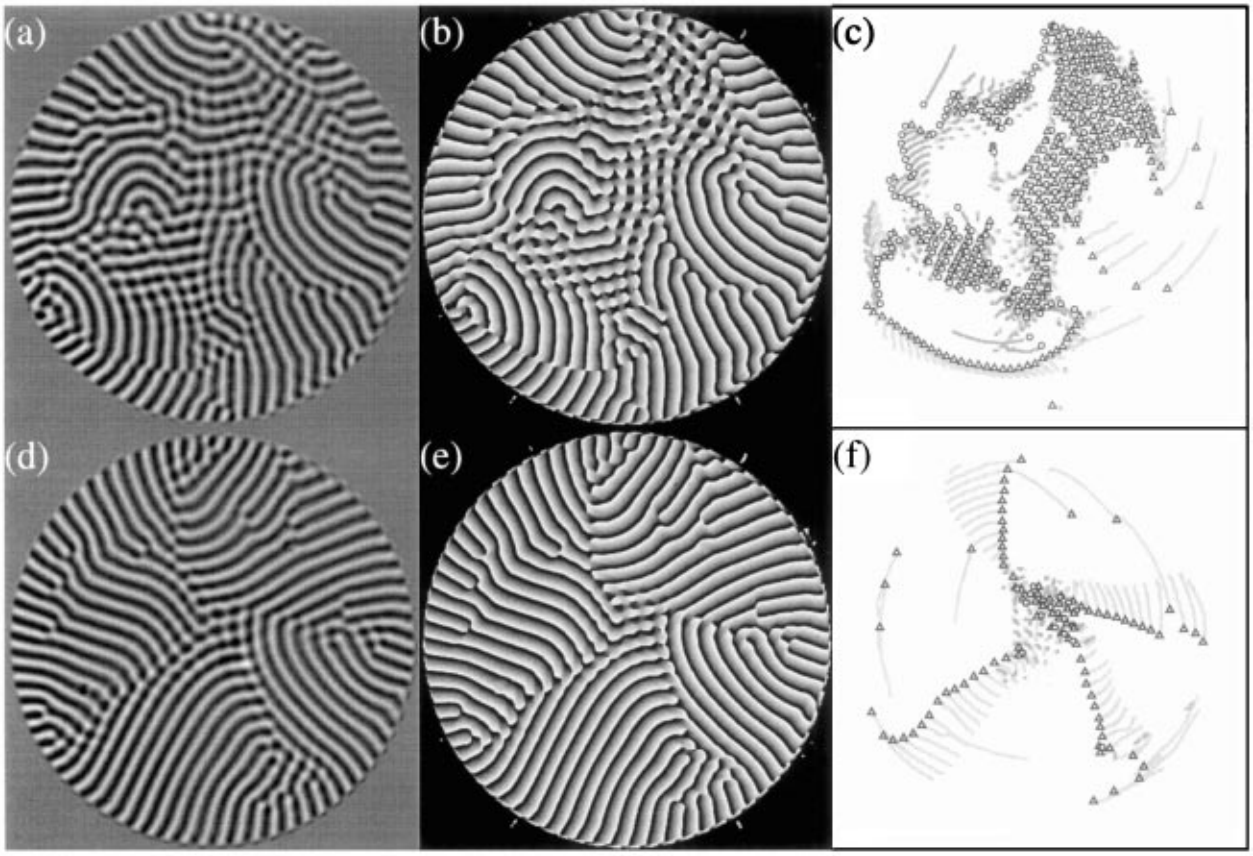

FIG. 1. Convection patterns recorded (a) 510τ and (d) 1530τ after convection was initiated. The phase of the complex order parameter is shown in (b) and (e) with the interval $0 \rightarrow 2\pi$ mapped to grayscale for the patterns recorded at 510τ and 1530τ, respectively. Defects are mapped for the patterns at (c) 510τ and (f) 1530τ. In (c) and (f), phase defects for positive (negative) charge are indicated by circles (triangles) and the positions of the positive (negative) defects over the preceding 24τ are shaded light (dark) grey.

consisting of several domains of nearly straight rolls separated by well defined domain boundaries. Such a pattern is shown in Fig. 1(d). The ordered patterns exhibit global rotation, with all rolls moving in the same direction around the perimeter of the cell. Both clockwise and counterclockwise rotating patterns are observed to develop from the disordered initial patterns, but once the sense of rotation is established, it never reverses itself. It is our goal to characterize this transition by studying the evolution of phase defects in the pattern.

The first step in identifying defects in a TW convection pattern is to calculate the complex order parameter of the pattern as a function of time. The time series of each pixel in such patterns is oscillatory, and the structure of the pattern can be determined from the phase relationships between the pixels comprising the pattern [12]. The complex amplitude is calculated as a function of time and space by performing a complex demodulation of the time series of each pixel. The demodulation frequency is chosen to be the average of the oscillation frequency over the pattern. Figures 1(b) and 1(e) show the phase of the complex order parameter calculated from the patterns of Figs. 1(a) and 1(d), respectively.

One advantage of the phase representation of the pattern is that defects can easily be identified. A phase defect is defined as a point at which the amplitude $\|A\|$ of the order parameter vanishes, and the phase ϕ is undefined; it corresponds to the intersection of contours of $\mathrm{Re}(A) = 0$ and $\mathrm{Im}(A) = 0$, as shown in Fig. 2(e). The integral of $d\phi$ on a closed contour around the defect is equal to $2\pi n$, where n is the topological charge of the defect. In order to locate defects in the phase map, the topological charge is calculated at each pixel using a path consisting of the 8 surrounding pixels. A nonzero charge is found if a phase defect resides anywhere within the 3×3 block comprising the path. In general, there are several overlapping paths which contain each defect, so a connected group of pixels with the same nonzero charge is identified as a single defect.

The phase defects identified in the patterns of Figs. 1(a) and 1(d) are shown in Figs. 1(c) and 1(f). Defects with positive and negative charge are marked by circles and triangles, respectively, and grey shading indicates the trajectories of defects over the preceding 24τ.

Defects in the TW patterns typically appear in four basic configurations which are indicated in Figs. 2(a)–2(d).

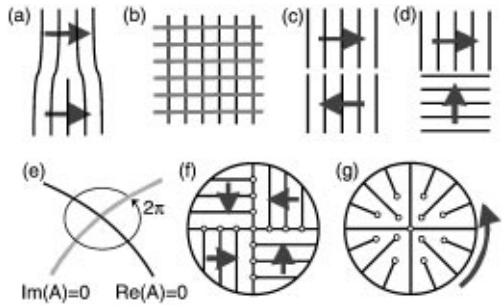

FIG. 2. Roll boundaries for defect structures found in TW patterns: (a) dislocation, (b) cross-roll area, (c) zipper boundary, (d) perpendicular boundary. (e) Sketch of a phase defect. Hypothetical TW convection patterns containing (f) domain boundaries or (g) dislocations.

Figure 2(a) indicates a simple dislocation. Numerous dislocations are visible within the large domains of traveling waves shown in Fig. 1(d), and a high-resolution image of a dislocation is shown in Fig. 3(a). In this structure, a single phase defect marks the termination of a roll. The dislocations are swept along with the convection rolls, and their large velocity is indicated by the long tails on the isolated defects in Fig. 1(f). Figures 2(c) and 2(d) indicate boundaries between domains of convection rolls. There is a region of overlap of the two wave components, and a row of defects of the same sign appears in this region. In the configuration of Fig. 2(d), which is most prevalent in the ordered patterns, the distance between defects is $2\pi/k$, where k is the wave number. A high-resolution image of such a boundary is shown in Fig. 3(d). The configuration of Fig. 2(c) is sometimes referred to as a "zipper," and has a defect spacing of π/k. There is a prominent zipper visible in the pattern shown in Fig. 1(a), and a high-resolution image of a zipper is shown in Fig. 3(c). Domain boundaries and dislocations contain a net charge, which cannot be created within the pattern, but must enter from the cell boundary.

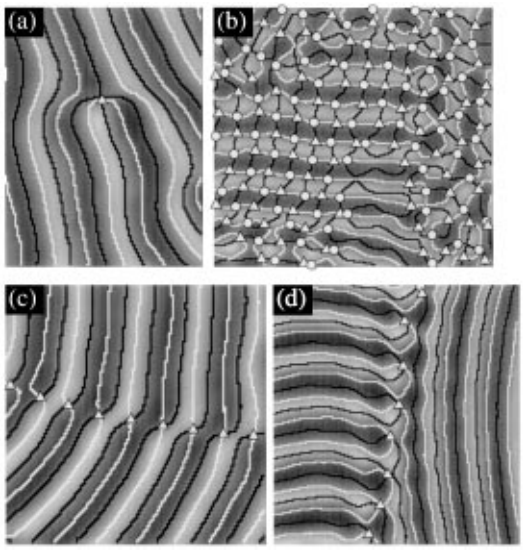

FIG. 3. Shadowgraph images of defect structures recorded in TW convection patterns. Contours of $\mathrm{Re}(A) = 0$ and $\mathrm{Im}(A) = 0$ are superimposed on the shadowgraph images, and phase defects of positive (negative) charge are marked by circles (triangles). Defects shown are (a) dislocation, (b) cross-roll, (c) zipper, and (d) perpendicular boundary.

The most complicated pattern element, indicated in Fig. 2(b), is the cross-roll area, in which mutually perpendicular standing waves alternate in time, for which the order parameter is of the form

$$e^{i(kx-\omega t)} + e^{i(-kx-\omega t)} + e^{i(ky-\omega t)} - e^{i(-ky-\omega t)}. \quad (1)$$

In this structure, defects of alternating polarity are observed on a square lattice with spacing π/k. The net charge of this structure is zero, although there are $(k/\pi)^2$ defects per unit area. A significant fraction of the pattern in Fig. 1(a) consists of this structure, as well as a small area at the center of Fig. 1(d). Figure 3(b) shows a high-resolution image of a large cross-roll area and associated defects at an instant when horizontal rolls have superseded vertical rolls. Since these structures have no net charge, they can spontaneously appear and disappear from the bulk of the pattern via the creation and annihilation of pairs of oppositely charged defects.

Cross-roll areas are not stable, but appear to be sustained by the collision of traveling waves. Disorder in TW patterns typically takes the form of defect-rich but neutral cross-roll areas in which the individual wave components have nonuniform time-dependent amplitudes. Therefore a large number of defects with no net charge is an indicator of disorder in these TW patterns.

The width of the wave-number distribution of the convection pattern as well as the statistics of defects are plotted as a function of time in Fig. 4. Initially, the pattern contains about 600 defects, with a net charge close to zero. This corresponds to 40% coverage of the pattern by the cross-roll structure. At first, the number of defects decreases rapidly, indicating rapid ordering of the pattern. This initial decrease in disorder is not reflected in the wave-number distribution shown in Fig. 4(a). At $t \approx 300\tau$, the number of defects stabilizes at about 300. Figure 1(a) shows a typical pattern from this period of persistent disorder. During the time interval from 300τ to 750τ, the total number of defects is relatively stable as the net charge steadily approaches a value of -72. There are 72 rolls around the perimeter of the cell, each of which terminates within the pattern and contributes a charge of ± 1, depending on its direction of propagation. (Rolls that begin and end within the pattern contribute a pair of oppositely charged defects and have no effect on the net charge.) Therefore the accumulation of a net charge of -72 means that all rolls are propagating in the same direction along the cell boundary, and this signals global rotation of the pattern. After global rotation is achieved, the total number of

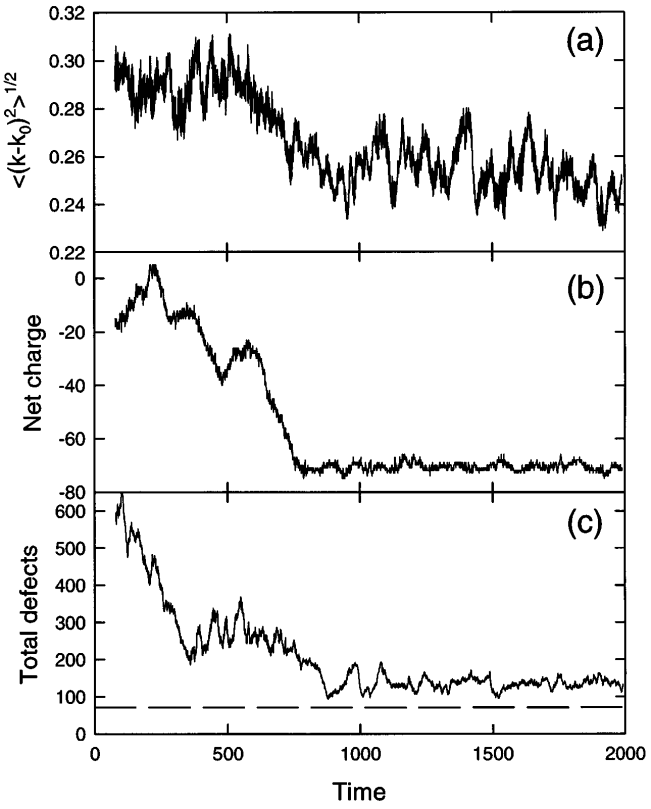

FIG. 4. Measures of disorder as a function of time during the transition from a disordered to a regular pattern. (a) The standard deviation of the peak in the structure function, where k is in units of h and $\bar{k} \approx \pi$. (b) The net charge of the phase defects in the pattern. (c) The total number of defects in the pattern. Defects attached to the cell boundary are excluded from the tabulation. The dotted line in (c) indicates the baseline of 72 defects (see text).

defects decreases to a minimum of about 100, indicating that there are only about 30 defects (15 pairs) in excess of the 72 defects which must be present. At this point the pattern has, in some sense, reached an optimum configuration; it has eliminated almost all extraneous defects and has selected a pattern in which the net charge has accumulated in domain boundaries [Fig. 2(f)] rather than in dislocations [Fig. 2(g)]. A slight sharpening of the wave-number distribution is also evident in Fig. 4(a) during the formation of the regular pattern.

Although the details of the pattern such as the initial number of defects and the direction of rotation vary from run to run, all of the runs share a common phenomenology. The initial ordering of the pattern stalls with 300–400 defects remaining (20% coverage), until a net charge of ± 72 accumulates. This is followed by a rapid collapse in the number of defects, suggesting that the ordering mechanism is facilitated by the state of global rotation.

In conclusion, we have described a state of defect-mediated disorder in binary fluid convection. We have demonstrated an algorithm for identifying and tracking defects in TW patterns, and we have shown that disorder in the system is marked by specific configurations of defects. The total number and the net charge of the defects are therefore an easily interpreted measure of the level of disorder in the pattern. Finally, we have used this technique to describe a transition from a disordered TW pattern to an ordered TW pattern. This transition is marked by a dramatic decrease in the number of defects, but only a slight sharpening of the wave-number distribution. We expect the technique described here will be applicable to any traveling-wave pattern, and it should be useful whenever spatiotemporal disorder is closely associated with the presence of phase defects.

We would like to acknowledge useful discussions with D. Ridgway. This work is supported by the U.S. Department of Energy under Grant No. DE-FG03-90ER14148.

[1] M. C. Cross and P. C. Hohenberg, Rev. Mod. Phys. **65**, 851 (1993).
[2] V. Steinberg, W. Moses, and J. Fineberg, Nucl. Phys. **B2**, 109 (1987).
[3] P. Kolodner, J. A. Glazier, and H. Williams, Phys. Rev. Lett. **65**, 1579 (1990).
[4] I. Rehberg, S. Rasenat, and V. Steinberg, Phys. Rev. Lett. **62**, 756 (1989).
[5] S. W. Morris, E. Bodenshatz, D. S. Cannell, and G. Ahlers, Phys. Rev. Lett. **71**, 2026 (1993).
[6] F. T. Arecchi, G. Giacomelli, P. L. Ramazza, and S. Residori, Phys. Rev. Lett. **67**, 3749 (1991).
[7] P. Coullet, C. Elphick, L. Gil, and J. Lega, Phys. Rev. Lett. **59**, 884 (1987).
[8] P. Coullet, L. Gil, and F. Rocca, Opt. Commun. **73**, 403 (1989).
[9] H. Xi, J. D. Gunton, and J. Vinals, Phys. Rev. Lett. **71**, 2030 (1993).
[10] Y. Hu, R. E. Ecke, and G. Ahlers, Phys. Rev. Lett. **74**, 391 (1995).
[11] W. Barten, M. Lücke, M. Kamps, and R. Schmitz, Phys. Rev. E **51**, 5636 (1995).
[12] A. La Porta and C. M. Surko, Phys. Rev. E **53**, 5916 (1996).